

	
Project (Grant) Number:	824135
Project Acronym:	SOLARNET
Project Title:	Integrating High Resolution Solar Physics

Document Details	
Document Title:	Field Splitter Design and Microlens Specification for a Microlensed Hyperspectral Imager
Prepared by (Institution’s Name):	Max Planck Institute for Solar System Research (MPS)
Work Package number & Title:	WP6 - Advanced Instrumentation development sWP6.2 Microlens spectrograph
Deliverable Number & Title:	D6.7 - Field Splitter Design and Microlens Array Specifications
Serial Number of Deliverable:	D61
Document code: (inserted by project office)	D6.7_Version 1.0
File name: (inserted by project office)	SOLARNET_D6.7_V1.0_FSD_Public_20200226
Date uploaded: (inserted by project office)	Feb 26 th , 2020

AUTHORS/ CONTRIBUTORS LIST

Name	Function	Organization
Michiel van Noort	Sub-WP leader	MPS

SCIENTIFIC APPROVAL CONTROL FROM SUB-WP & WP LEAD

Control	Name	Organization	Function	Date
Prepared	Michiel van Noort	MPS	Sub-WP leader	Feb 18 th , 2020
Approved	Manolo Collados	Instituto de Astrofísica de Canarias (IAC)	WP6 leader	Feb 24 th , 2020

ADMINISTRATIVE APPROVAL CONTROL FROM PROJECT OFFICE

Control	Name	Organization	Function	Date
Approved	Tirtha Som	Leibniz-Institute for Solar Physics (KIS)	Project Manager	Feb 25 th , 2020
Approved	Rolf Schlichenmaier	KIS	Project Coordinator	Feb 25 th , 2020
Authorized	Markus Roth	KIS	Project Scientist	Feb 26 th , 2020

HISTORY OF DOCUMENT CHANGES

Issue	Date	Change Description
Version 1.0	Feb 26 th , 2020	Initial Issue

Table of Contents

Table of Contents	3
Introduction	4
1. Microlensed Hyperspectral Imaging.....	4
2. Splitting concepts	6
3. Optical splitting designs.....	8
3.1. Micro-splitting	8
3.2. Macro-splitting	10
3.3. Splitter Selection	11
4. Microlens array.....	11
4.1. Numerical model	13
Summary.....	14
References.....	14

List of Abbreviations

FOV	Field of View
MLA	Microlens Array
SST	Swedish Solar Telescope
fps	frames per second

Introduction

To understand the physics of the outer solar atmosphere, the only reliable information that we can realistically expect to make use of are remote observations of the solar surface. Such data carry information about the local conditions in the outer layers of the solar atmosphere, through wavelength dependent variations in the intensity and polarization, caused by energy transitions of the atoms and molecules that constitute our local star.

Unfortunately, the mapping of the local atmospheric conditions to the observed emergent spectrum is non-linear and non-unique, presenting anyone wishing to convert an observed spectrum back to the atmosphere by which it was generated with a formidable task. Not only is the problem ill-posed, due to the non-unique and non-linear mapping, the non-local character of the radiative process in the solar atmosphere severely limits the information contained in a given atomic line transition.

It is therefore of critical importance to observe the emergent spectra with the highest possible spatial, spectral and time resolution, using a well-characterized instrument that allows for the data to be restored to their original appearance, and thereby maximize the accuracy and amount of information that can be extracted from them.

To this end, a prototype integral field instrument, the Microlensed Hyperspectral Imager (MiHI), was designed and built as part of the first SOLARNET project. The prototype was built as a plug-in to the existing TRIPPEL spectrograph, currently installed at the 1-meter Swedish Solar Telescope (SST), and has been operational since October 2016. Data were recorded over a number of observing campaigns, in three different wavelength bands, containing the Na-D1 line at 589nm, a pair of highly magnetically sensitive Fe lines at the design wavelength of 632nm, and the H-alpha line at 656nm.

Due to their unusual format, the conversion of the raw data to a science-ready end product has required significant new developments in the areas of data reduction and image restoration. Although these developments have not yet been completed, a preliminary data reduction pipeline now exists, allowing for the routine reduction of datasets recorded with the prototype. These data are of high quality, and provide access to a new regime in sensitivity and cadence, that cannot be achieved with more traditional instrumentation.

Unlike traditional imaging spectrometers that need to scan at least one dimension of the parameter space (wavelength or one spatial dimension), hyperspectral imagers capture the entire information content within their field of view at once, which requires a much larger number of available detector pixels. This is challenging both optically and from a detector point of view. If the instrument is to overcome its limitations, a way needs to be found to distribute the information over multiple detectors.

1. Microlensed Hyperspectral Imaging

The Microlensed Hyperspectral Imager is an integral field spectrograph that makes use of a double sided microlens array (MLA) to re-format a focal plane image into an array of point sources, thus generating a focal plane image of which a large fraction is not illuminated. This space is then used by a spectrograph, mounted behind the MLA, that disperses the light in the dot into a spectrum.

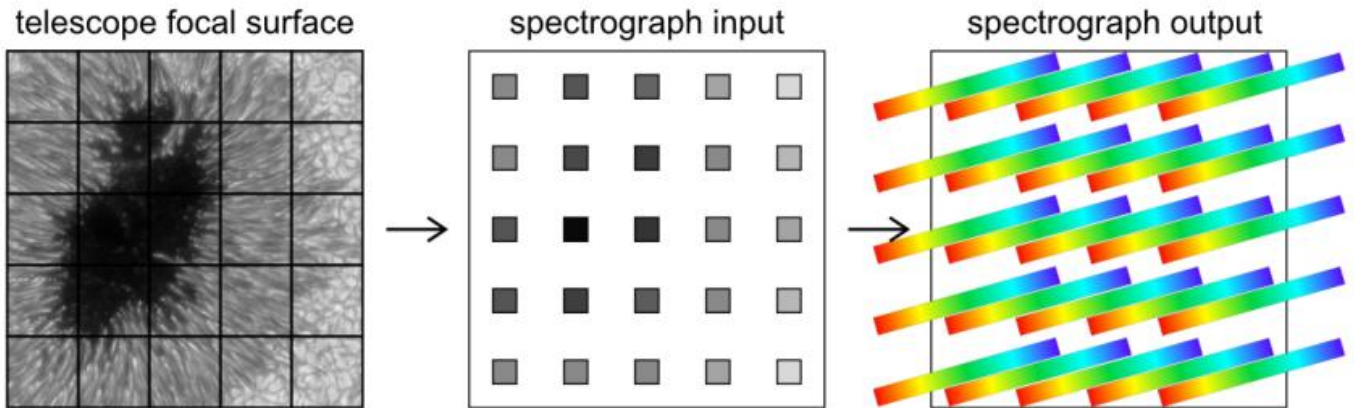


Figure 1: MiHI principle of operation: the image is sampled by microlenses (left), then demagnified (middle), so that it can be dispersed (right)

A narrow-band prefilter is then placed in front of the instrument, to avoid overlap of the individual spectra with the spectrum of any of the neighbouring image elements. The MLA of the prototype instrument developed in SOLARNET1 consists of 128x128 individual 2-lens re-imaging systems, generating enough dark space to accommodate 324 spectral pixels, covering a spectral band of approximately 4Å.

The data produced by this prototype contains spectral information, interleaved with spatial information, as shown in Figure 2. A critical step in the data reduction is the calibration of a coordinate map, that maps each coordinate in the hyperspectral cube to a detector coordinate, so that the 3D cube can be extracted.

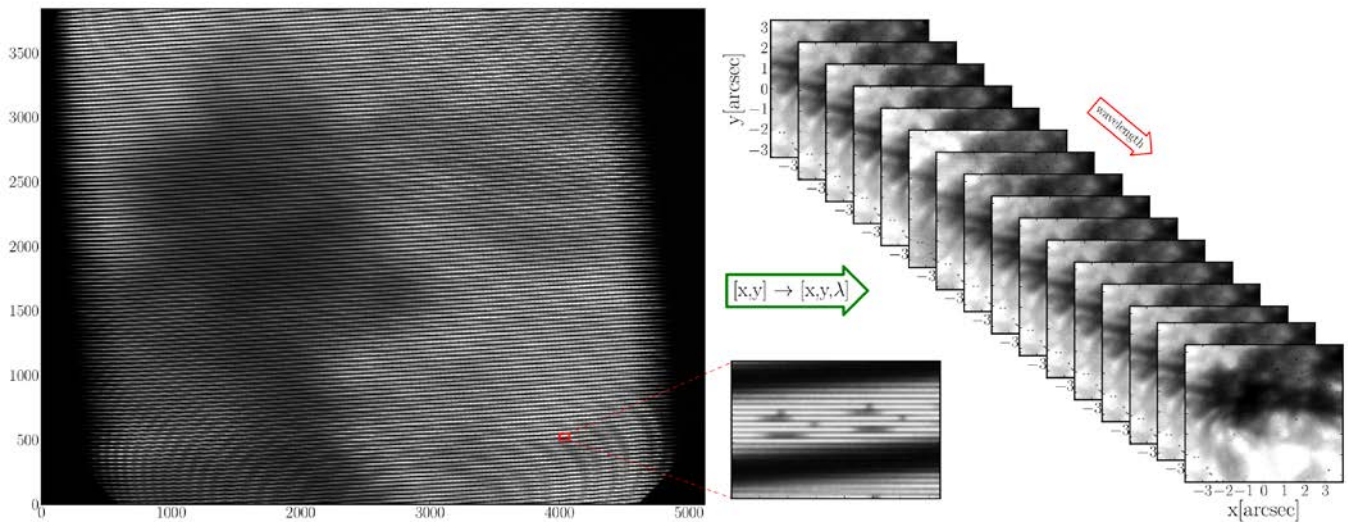


Figure 2: Raw MiHI data frame at 630nm, mapped to a flatfield corrected 3D cube

For the data recorded so far, it was possible to use telluric lines, originating in the Earth's atmosphere, to trace known coordinates in the hyperspectral cube to the detector, and build up the map from there by iterative refinement.

Once the data are mapped, image restoration can be used to restore the data to their original resolution. This was done using a context camera, that records the image falling on the field selector of the instrument, and can see both the context of the selected field, as well as the field itself. These data are first used to

restore the context image itself, but can also be put to good use in the restoration of the spectral data, using the spectral restoration technique by van Noort (2017).

An example of a restored dataset is shown in Figure 3. The 128 image elements are critically sampling the focal plane, resulting in a FOV of 7.3x8.2 arcseconds. The spectral resolving power, at more than 300000, is excessive, and results in a rather small spectral range of only 4Å.

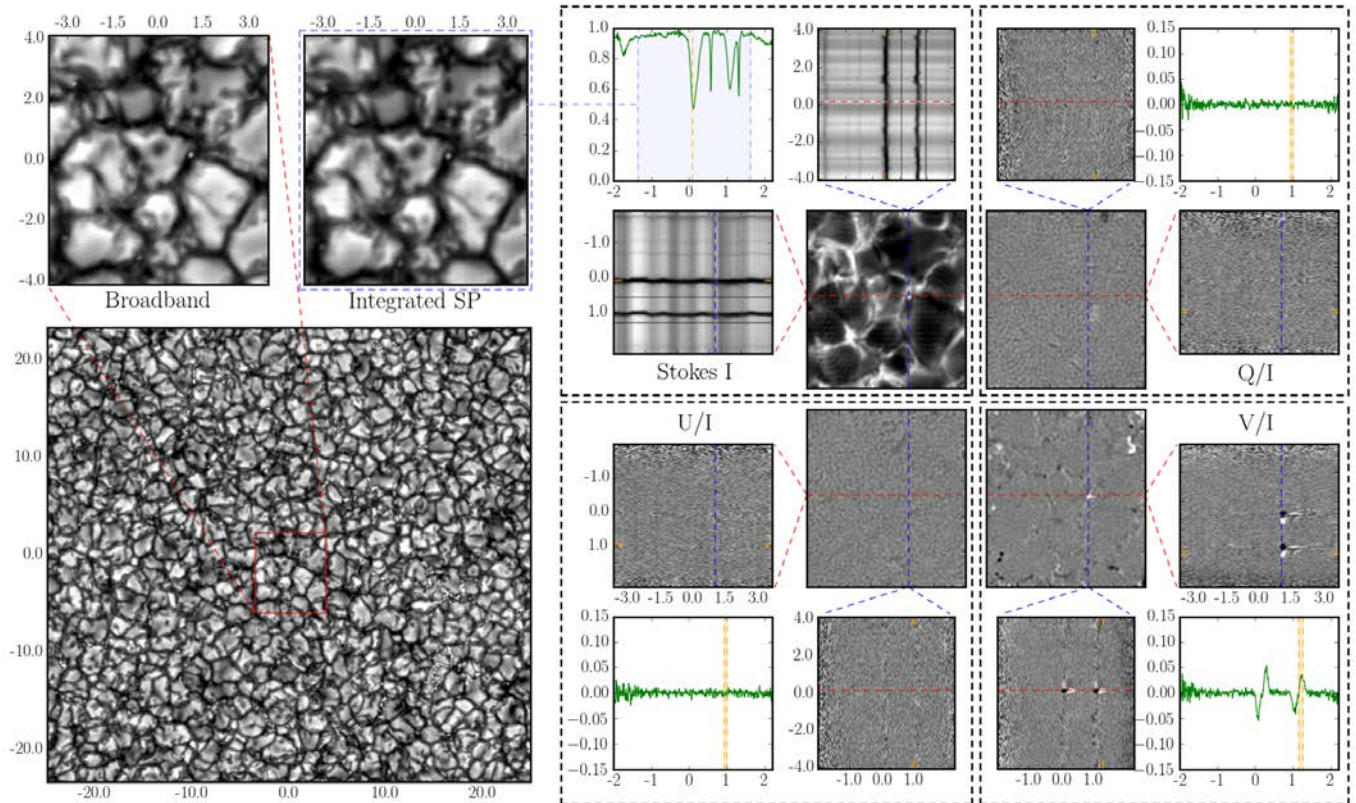


Figure 3: Restored MiHI dataset at 630nm

Clearly, although the spectral and spatial resolution are high, the FOV is small, and the spectral range is very limited.

For a 1m class telescope, such as the SST, these limitations are significant, but they are acceptable considering the improvements in cadence and sensitivity of the data. For larger aperture telescopes, however, the situation is not the same. For the next generation solar telescopes, with apertures of 4m or more, the required size of the field will be 4 times larger, while covering the same angular size on the Sun.

2. Splitting concepts

The splitting of the field can be carried out for a number of different reasons, that have an impact on the most logical realization.

If the reason for splitting is the unavailability of an appropriately dimensioned image sensor, it may be preferable to split the field in front of a single instrument that is able to accommodate a large FOV, so that all instrumental properties are shared between the subfields. This may have the advantage that if the instrument is tuned, this is done for all fields simultaneously, and all instrumental properties will most likely

vary smoothly across each field, and from field to field. Avoiding variability of the instrumental response altogether, however, is not realistic, since there is always a contribution of the image angle in the pupil to the angle on the grating, causing the spectral dispersion to vary over the FOV.

It is also possible that the optical design itself is the reason for splitting the field, in which case each field must be sent to another instrument, with its own individual characteristics. This is the case when the optical FOV cannot be made sufficiently large to accommodate the coveted FOV and spectral range, without compromising the instrumental performance.

Which one of these two reasons dominates determines what the best method for splitting is. If the instrument is sufficiently large, but the sensors are not, the optical splitter must be designed such that a common pupil is retained for all of the subfields, otherwise the instrument properties will not be similar for all fields. If on the other hand a number of separate instruments are built, each instrument can be individually aligned with the pupil of each subfield. Although this does not exclude the use of a common pupil, it is not a hard requirement.

The design of a Microlensed Hyperspectral Imager relies on a primary re-imager (see Figure 2) for adapting the image scale from the plate scale on the optical bench of a typical solar telescope, to that dictated by the image element size of the MLA. Splitting can be accomplished before, or after that re-imager, it can even be an integral part of it.

The precise placement of the splitting optics has a significant impact on the splitting properties, and must be carefully considered. Splitting before the re-imager (micro-splitter) is more likely to lead to optical artifacts, since the scale of the optics relative to the wavelength is relatively small, leading to a potential for diffraction effects. Such effects can be minimized by splitting close to a focal plane, and has the advantage that the optics is typically small, and can be produced using well-established techniques for micro-structuring of surfaces, such as ion-beam etching. A significant advantage of such manufacturing methods is that the fabrication of a parallel array of nearly identical elements is very easy, so that splitting in a large number of fields is trivial to accomplish. Achieving a common pupil for a parallel array, however is not a simple task, and will be explored in an optical design below.

Splitting after the re-imager (macro-splitter) is a much easier task, because the optical properties of a large F-ratio beam are considerably more benign than those of a low F-ratio beam. This means that the optical performance of such a splitter is much easier to optimize than that of a micro-splitter, but the splitter itself must consist of much larger optical elements. This makes it more difficult to split in many fields, which now requires a number of large precision optical parts, with nearly identical properties, although they can be plane.

In the following, we will investigate an optical design for both of these splitting concepts. We will assume a single instrument will be used, and that only the image sensor is segmented, because this is the most demanding situation from an optical point of view, whereas for a fully segmented instrument, the required common pupil, although not required, is not a disadvantage.

3. Optical splitting designs

We now evaluate two optical splitting concepts, a micro-splitter and a macro-splitter. Both will be required to have a common pupil for all subfields, so that it can be used in a single instrument. The discussion is in relatively general terms, so that a number of different aspects can be discussed, without loss of clarity to details.

3.1. Micro-splitting

A micro-splitter for use on a single hyperspectral instrument carries out the splitting of the focal plane before adjustment of the image scale to that required by the MLA of the hyperspectral imager. The first task is to separate the individual fields in the focal plane, which is most conveniently done by placing an MLA in the focal plane of the telescope.

Because the array of microlenses then forms individual images of the telescope pupil at its focal length behind each element in the array, the emerging beam is not suitable to be sent through a single instrument, since the array of pupils will probe the instrument in different ways, thus potentially affecting the instrumental response for the different segments in unpredictable ways.

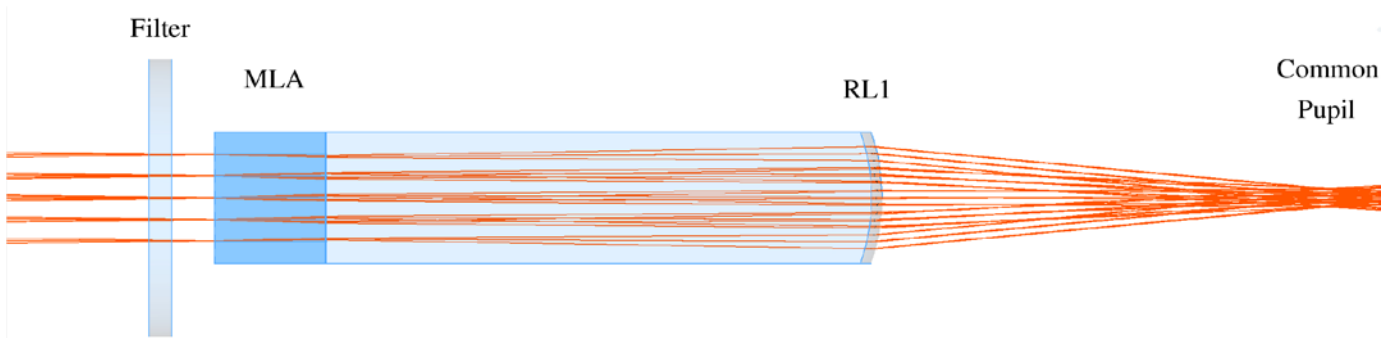


Figure 4: Micro-splitting array: a double sided MLA reduces the beam diameter of each segment, all of which are then converged by a global lens to form a single pupil.

To avoid this problem, the beams of the sub-images must be converged, so that they cross in a single location, which must coincide with the location where the pupil of each individual image element is formed. Redirecting the beams of the MLA elements to a single location can be achieved by using individually adjusted refractive wedges, that deflect the light at just the right angle, which requires an array of individually angled prisms. Although these wedges accomplish the task of deflecting the beams of all elements towards a common pupil, no common pupil is formed, because the distance to the common location is not identical for all MLA elements. To achieve a common pupil, a compensation of these path length differences to the common location is required, which can be conveniently accomplished by adjusting the wedge thickness.

To eliminate the need for individualized image elements, and simultaneously address the problem of the required increase in the distance to the pupil as a function of the distance to the optical axis, we can make use of a common plano-convex surface for all elements of the MLA, and compensate for the curvature this introduces by using a second MLA. The macroscopic and microlens surfaces combine to form the refractive wedge, and the sag of the common surface adjusts the optical path length to the optical axis for all MLA elements, thus making it possible to form a common pupil.

Figure 4 shows the basic optical design of such a solution, with an array of 4x4 segments. The final surface of the device, RL1, is aspherical, without which it is not possible to form a common pupil. The F-ratio of the beam emerging from RL1 cannot be made too low, or the ability to produce a common pupil is lost. To

achieve a large magnification, however, this can lead to a relatively long re-imaging system of 1500mm or more, and require a large re-imaging lens.

With this solution, a good optical performance can be achieved, and splitting in excess of 4x4 segments is possible, as shown by the spot diagrams of such a system, however, distortions are a problem if a single output plane is required. Figure 5 shows such a configuration, in which a single lens, RL2, forms a tightly packed array of image segments.

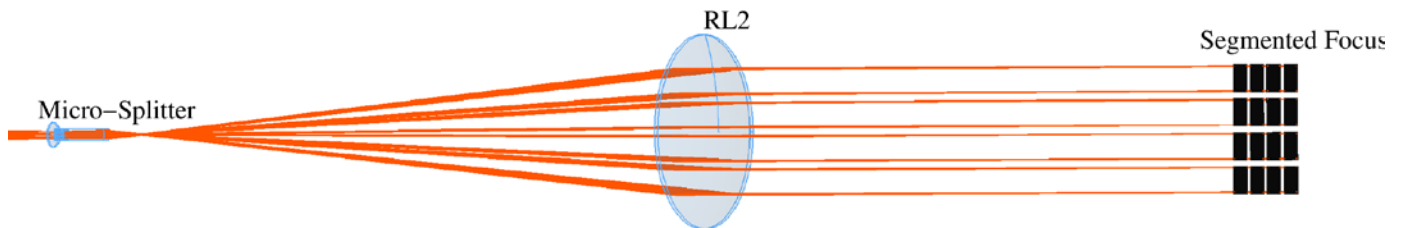


Figure 5: Single re-imaging lens primary re-imaging solution, with integrated segmentation array. A single lens is used to re-image all segments onto a single focal plane.

An example of the spot diagrams for a central segment is shown in Figure 6, showing that the optical performance of this configuration is close to diffraction limited, which is the case for all 16 fields, and shows no significant deviation from this behaviour for the wavelength range from 400 to 630nm, although there appears to be a clear dependence of the distance to focus on wavelength.

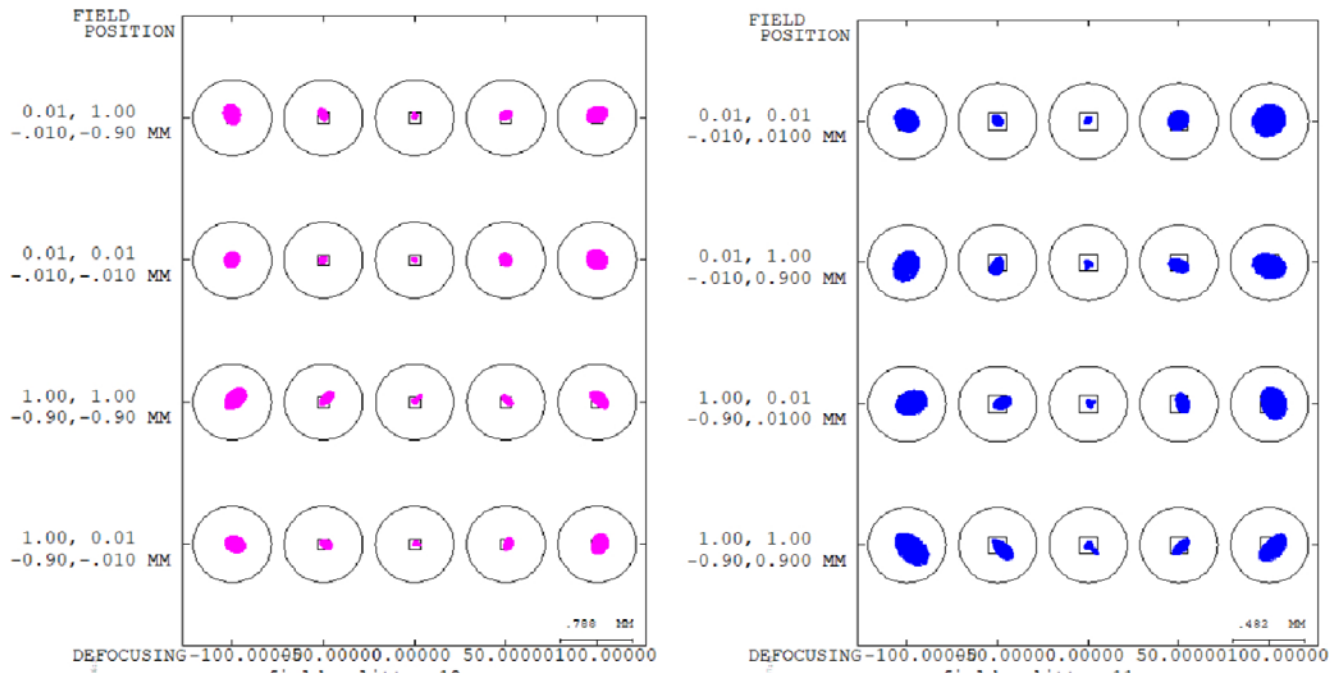


Figure 6: Spot diagrams of a single lens splitter configuration at 6320nm (left) and 400nm (right). The diagram shows close to diffraction limited performance, indicated by the spread of the trace points relative to the diffraction limit (indicated by the circle).

The separation between the subfields is approximately 8mm, sufficient to fold the beam in any desired direction by using a plane mirror, and feed it into an array of instruments. The large diameter of the re-imaging lens of nearly 200mm is a real concern though, as is the onset of geometric distortion for fields in excess of 4x4 segments.

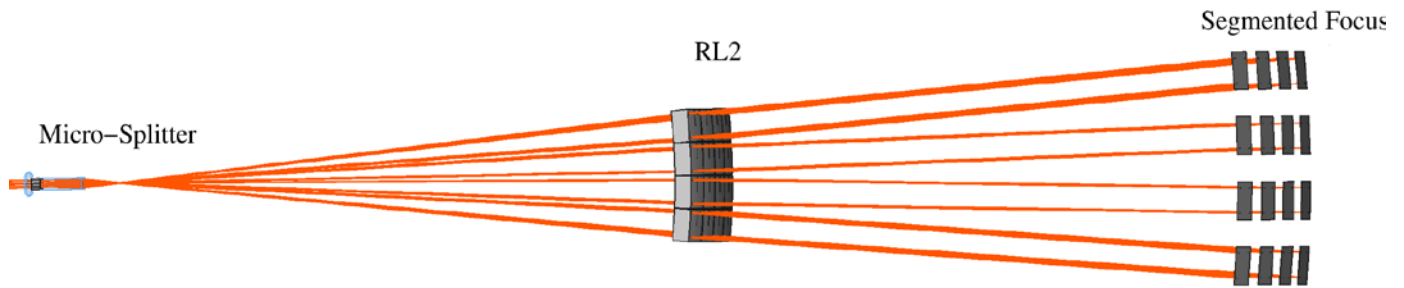


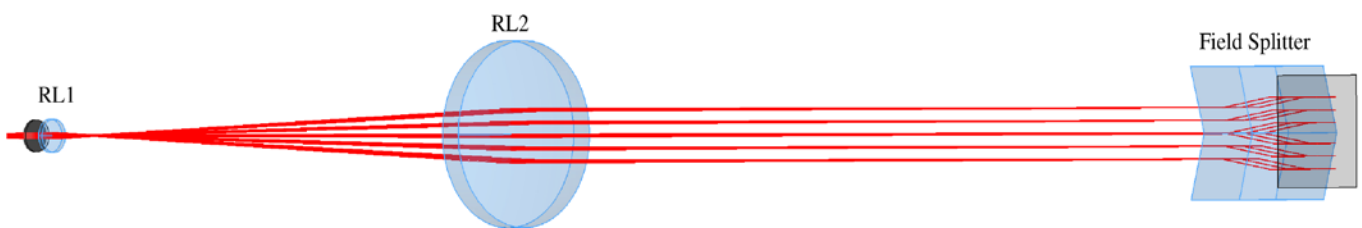
Figure 7: Divergent primary re-imaging solution. The same micro-splitter is used as in Figure 4, but instead of a single re-imaging lens, an array of lenslets is used to keep the optical system on-axis. As a result, the segments diverge from the optical axis

A solution can be found that has nearly no geometric distortion, by making use of an array of lenses that are radially placed with respect to the common pupil, as shown in Figure 6. Although this system is optically on-axis downstream from the micro-splitter, the optical performance is actually poorer. Moreover, the dispersion of the micro-splitter causes the radial divergence of the segments to be wavelength dependent, so that a clear shift can be seen between the 400 and 630nm segments on the MLA.

The relatively achromatic behaviour of the common lens configuration can be understood by considering that locally the effect of RL2 is similar but opposite to that of the refraction wedge applied by RL1, which is nearly independent of wavelength as long as RL1 and RL2 are made of the same material.

3.2. Macro-splitting

Compared to the micro-splitting solution, the macro splitter is much simpler, and can exist only by virtue of the very high F-ratio of the beam that is produced after the primary re-imager. To split the focal plane, each image segment is refracted away from the optical axis using an inclined glass plate, with a different inclination angle for each of the segments.



An inclined glass plate is well known to induce strong astigmatism in a converging beam, causing an elongation of the PSF of the optical system. In this case, however, with an F-ratio that is sufficiently large, this effect is completely negligible, even though the thickness and angle of the plate are considerable. This can be seen in Figure 8, that shows the field splitting device, together with the spot diagram, that shows no sign of an asymmetric aberration, even in the presence of a large defocus term.

A similar problem with chromatic changes to that in the micro-splitter occurs here. Since the material of the splitter is not free of dispersion, the beam is refracted over an angle that is wavelength dependent, and therefore the position of each segment on the MLA will vary with wavelength.

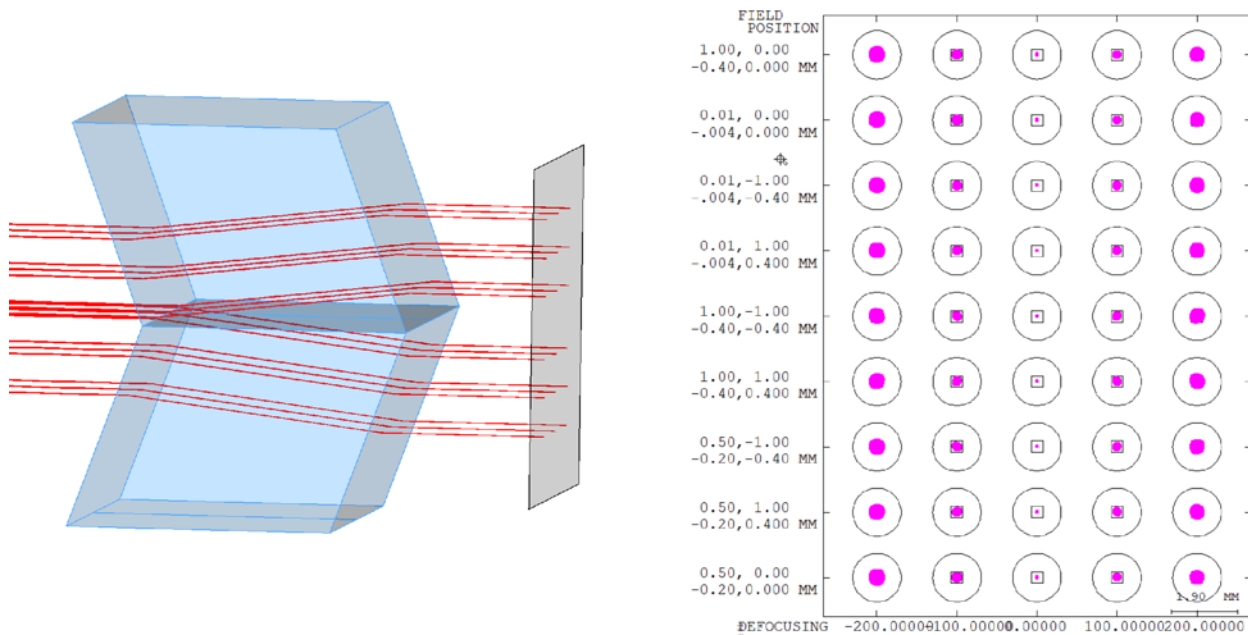


Figure 8: Zoom of a ray-trace of the scaled beam with a macroscopic field-splitter device installed (left). Despite the large thickness and angle of the glass, the optical performance is not compromised at all, as indicated by the very compact spot diagram of the beam after the splitting device (right).

It is possible to avoid this problem partially, by combining two materials, with different dispersion properties, which reduces the displacement, but it can be eliminated only for two specific wavelengths.

3.3. Splitter Selection

Although it would be desirable to create a splitter design that is scalable and has good optical properties, the complexity of such a design is relatively high, and requires custom designed micro-optics. The overall number of surfaces is similar to the macro-split option, but it does not grow with the number of image segments. Chromatic effects are largely compensated in a common pupil, single lens instrument, but if many segments are required, the physical size of the magnified, segmented focal plane becomes problematic. The obvious solution, individual re-imaging of each image segment, requires many much smaller lenses, advantageously distributes the fields radially, but is no longer chromatically compensated, causing a wavelength dependent shift and shift of the focal plane.

The macro-split option is exceedingly simple, and introduces only two extra surfaces, both of which are plane. The large construction it requires comes at a cost, both in monetary and optical terms, but this is offset by the significant advantages in optical surfaces and tolerances. The design works for all wavelengths, but causes a wavelength dependent displacement.

Since the aim of the current project is to study the concept of recording and restoring a split field dataset, and not to design a fully functional field splitter for a multi-segmented instrument, we select the macro-splitting solution as the most obvious choice for the current project, since it has the highest optical performance, and is the least likely to put strong demands on alignment accuracy and surface quality.

4. Microlens array

The MLA that was used in the prototype study was designed to match the TRIPPEL spectrograph that it was built for. This meant that the F-ratio of the beam emerging from the MLA elements was required not to be lower than the minimum of 13 that the spectrograph was designed for. This sets a firm lower limit on the

pitch of the MLA, the optimum of which was determined to be around 325 μ m. With such a large pitch, the FOV of the spectrograph was unable to hold more than 128 image elements, severely limiting the size of the FOV on the Sun that could be observed.

For the present evaluation, we start with a clean slate, so that the imaging properties of the hyperspectral instrument, or whatever takes its place, can be selected to have any value we want. To select the optimum MLA pitch, we start by selecting the camera that we wish to use, and in particular the physical size of the pixels of the image sensor.

We start by selecting the largest format image sensor currently on the market, capable of at least 30fps, and with good QE and noise characteristics. The best choice at the time of writing is the AMS/CMOSIS CMV50000, a 48Mpx sensor capable of 30 fps, with an rms readout noise of only 8.8e-. This sensor has a 4.6 μ m pixel pitch, which is the starting point for the definition of the MLA.

To sample the image plane appropriately, the pixel size, d , of the camera requires the optical system that provides it with an image to have a specific F-ratio, approximately given by $d = \lambda F/2$, where λ is the wavelength of the light. For $\lambda = 650\text{nm}$, and a pixel size of 4600nm, the appropriate F-ratio of the beam evaluates to a value of 14.1. However, because the instrument beam is dominated by diffraction effects, the illumination of the pupil is not homogeneous, but has a radial illumination variation, with a beam profile close to that of a Gaussian beam. This increases the effective F-ratio of the beam, as compared to the actual F-ratio, by a factor of approximately 2, so that to keep the sampling of the focal plane by the selected image sensor close to critical, we need the F-ratio of the beam to be around 7. This means that, provided that the hyperspectral imager is designed accordingly, optimal optical performance is achieved when the emerging beam from the MLA has an F-ratio that is not lower than that imposed by the pixel size.

To design an MLA that outputs the desired beam properties, we need to consider the wavelength, and the spectral range that we require. If we aim for an optimal performance over the visible part of the spectrum, a wavelength limit must be selected, above which the instrument will inevitably lose efficiency. For a wavelength limit of 650nm, we wish to produce an F-ratio after the MLA not less than 7.

If N^2 spectral elements are required, we must reduce each image element by a factor N , not taking into account the separation between the spectra required to minimize spectral contamination, and the additional spectral elements needed to separate the spectra of subsequent image rows. The typical value for N is about 16, which should yield 256 spectral elements.

The dominant effect controlling the F-ratio of the emergent beam is the effect of diffraction on the edges of the microlenses on the front side of the array. The severity of the diffraction is determined by the MLA pitch d , and scaled up by the scale factor N . If we want the whole central diffraction maximum to propagate through the instrument, we must have $2 N \lambda/d > 1/F$

Assuming $N=16$ and a wavelength of 650nm, an output beam with an F-ratio of 7 is produced by an MLA pitch d of approximately 150 μ m.

4.1. Numerical model

The approximate derivation above assumes that the light incident on the front side of the MLA is perfectly plane, which in reality it is not, and assumes that the image of the front side lens onto the detector is a point of zero size. In reality, the image is not a point source blurred by diffraction, but it is slightly broader, leading to overlap between the individual spectra.

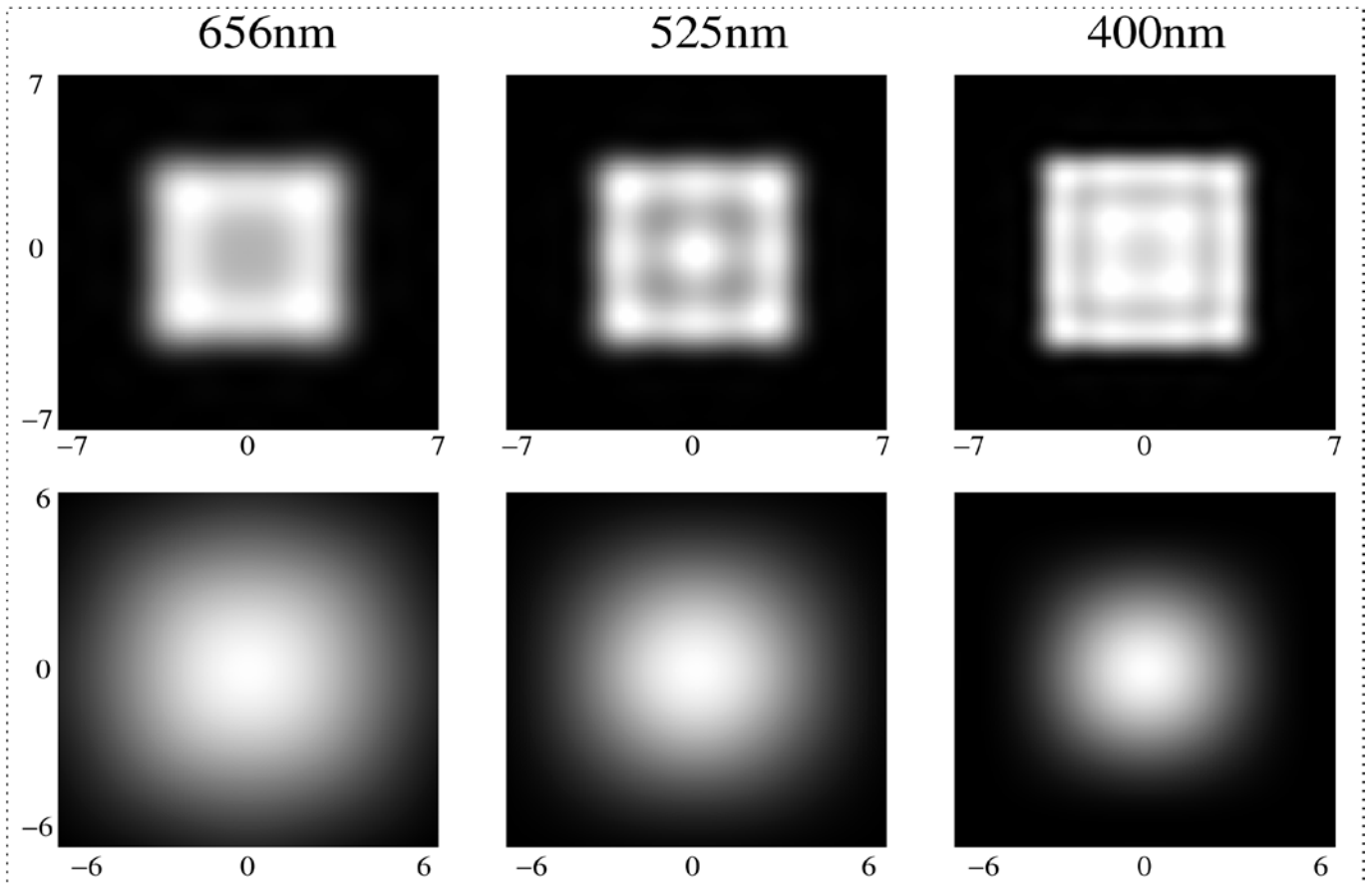


Figure 9: Simulation results of numerical simulated wave propagation of a plane wave through an MLA element of 160x160um. The top row shows the re-imaged front side of the MLA element, serving as the input for the hyperspectral instrument, the illuminated area covers approximately 7x7um, and will be re-imaged onto the image sensor, but significantly broadened by diffraction. The bottom row is the illumination pattern of a 12.5x12.5mm plate, placed at 100mm distance from the MLA. Full illumination of the plate is achieved for an F-ratio of 8. The calculations were carried out for a wavelength of 656nm (left), 525nm (middle) and 400nm (right), clearly showing the wavelength dependence of the F-ratio on the wavelength.

To model these effects in detail, the propagation of the light through the optical system must be calculated using an EM wave description of the light. For this, a computer code was developed that solves the propagation of the light through the microlens system by calculating the electric field in a sequence of planes in the optical system, by numerically evaluating the Fresnel diffraction integral. The integral applies Huygens principle to every point in a source plane, and calculates the amplitude and phase of the electric field in a point in a destination plane, by integrating over the electric field contributions from each point in the source plane individually. By considering multiple angles of incidence of the incoming light on the MLA and integrating over them with the proper weight, the effect of the finite F-ratio of the incoming beam can be taken into account.

The simulations indicate that the size of the re-imaged front side lens adds about 50% to the size of the image created by a single MLA element, and that the scale factor therefore has to be increased to

approximately 24. This decreases the F-ratio of the emerging beam, which has to be compensated for by increasing the pitch of the MLA.

The optimum solution, where all effects were taken into account as much as possible, was found experimentally, and is shown in Figure 9. The effect of the wavelength on the F-ratio of the beam is clearly visible in the bottom row. The 7x7um input image of the light entering the front side of the MLA is re-imaged by the hyperspectral instrument to a blurry dot, due to diffraction effects. Because the F-ratio scales with the wavelength, the image resolution on the sensor is independent of wavelength. The optimum values of the MLA for the selected sensor are given in Table 1

Table 1: Optimum values for an MLA matching the pixel size of the CMV50000 image sensor

Pitch	160um
Radius front side lenses	952.615 um
Radius back side lenses	40.9 um
Thickness	3098.87um
Substrate	SiO ₂
Scale factor N	22.86
Width x Height	256 x 256 elements (40.96x40.96)

Summary

We have investigated the possibilities for splitting an image in a focal plane into multiple segments, to be sent through one large, or multiple smaller hyperspectral imagers. Two approaches were studied: a micro-splitting option, taking place before the adjustment of the image scale to the MLA of the hyperspectral instrument is made, and a macro-splitter option, which is inserted into the beam close to the MLA. Both concepts can produce a segmented focal plane, and when integrated with the re-imaging optics, with nearly diffraction limited optical performance.

The micro-splitter has the notable advantage that it is easily able to produce 3x3 or 4x4 arrays of image segments of good optical quality, using relatively simple optics. It does, however, suffer from some chromatic effects that require a significant re-focus when the wavelength is changed.

The macro-splitter has outstanding optical performance, and is exceedingly simple to implement. It is unclear, however, how well it will scale well to many image segments, and requires heavy glass elements with large polished surfaces.

The task of this sub-WP is to develop a multi-segment strategy for enlarging the FOV of hyperspectral imagers. Since the difficulties anticipated for many segments do not differ substantially from those expected for only two segments, the macro-splitting solution is to be preferred, for its superior optical characteristics and lower complexity.

The appropriate MLA, proportioned specifically to match the pixel size of currently the best available image sensor on the market, was modelled and specified.

References

2017, van Noort, *Astronomy & Astrophysics*, 608, id.A76, pp.